

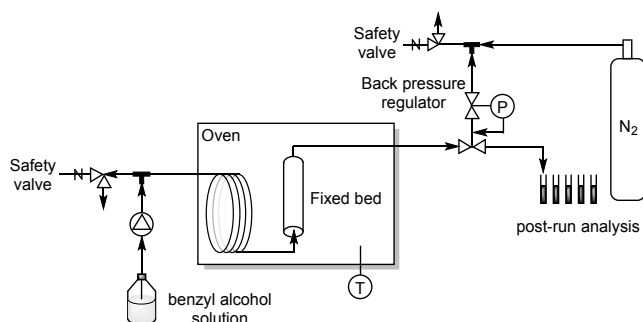
Supporting Information

Continuous Flow Aerobic Alcohol Oxidation Using Heterogeneous Ru⁰ Catalyst

Julien Sofack Kreutzer,^a Laurent Vanoye,^a Boris Guicheret,^{a,b} Régis Philippe,^a Estelle Metay,^b Marie-Christine Duclos,^b Marc Lemaire,^b Claude De Bellefon,^a Pascal Fongarland,^a Alain Favre-Régouillon^{*a,c}

1. Experimental set-up for acceptor free dehydrogenation of benzylic alcohols.....	2
2. Possible elementary steps during the regeneration of Ru ⁰ from ruthenium hydride	2
3. Composition of the liquid phase as the function of the temperature.....	3
4. Thermodynamic approach used for O ₂ solubility prediction.....	3
5. Appreciation of possible mass transfer resistances	5
6. Determination of adsorption enthalpies through a liquid inverse chromatographic method	8
7. References.....	9

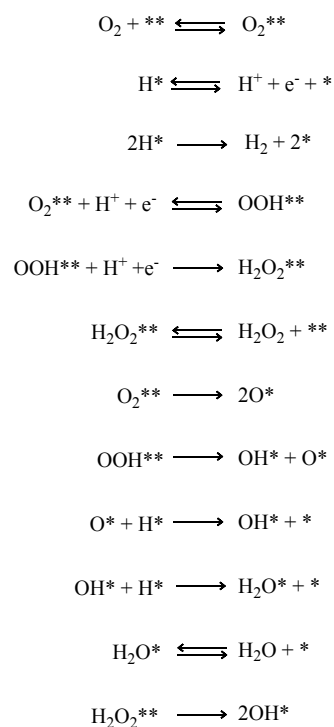
1. Experimental set-up for acceptor free dehydrogenation of benzylic alcohols



Scheme S1. General schematic of the G/L fixed bed reactor used for the acceptor-free dehydrogenation of alcohols

2. Possible elementary steps during the regeneration of Ru⁰ from ruthenium hydride

Scheme S2 depicts the series of steps that could lead to the formation of H₂O₂ and/or H₂O using catalysts in liquid solvents. These elementary steps have been described in literature during the direct synthesis of H₂O₂ and H₂O using Pd catalyst.^{1,2}



Scheme S 2 Plausible series of elementary steps for hydrogen peroxide and/or water formation during the regeneration of Ru⁰ from ruthenium hydride. A * denotes an empty site, X* represents an adsorbate bound to a single metal atom, X** signifies an intermediate adsorbed in an η² configuration. All reversible arrows represent a quasi-equilibrate step and each of the steps has its own rate constants. Scheme adapted from D. W. Flaherty *et al.*³.

3. Composition of the liquid phase as the function of the temperature

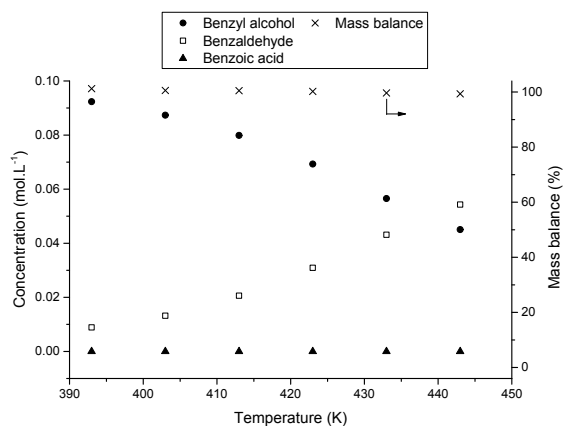


Figure 1. Composition of the liquid phase as the function of the temperature. [Benzyl alcohol]⁰=0.1 mol.L⁻¹ in tert-amyl alcohol, Q_{O₂}=49 NmL.min⁻¹, liquid flow rate=4 mL.min⁻¹, P=9 bar, T=393 to 433K. Reactor dimensions: length 136 mm and diameter 4.65 mm filled with 1.05 g of Ru⁰/γ-Al₂O₃ at 1 wt% of Ru.

4. Thermodynamic approach used for O₂ solubility prediction

Oxygen solubility in *tert*-amyl alcohol and solvent vaporization have been estimated numerically with PROSIMPLUS® software⁴ using G-L equilibrium flash calculations at constant temperature and pressure for a binary mixture of oxygen and *tert*-amyl alcohol. Calculations were done with the UNIFAC model in the different process conditions (T, P, inlet molar ratio). Typical results (Figure S 1) are given below for a pressure of 9 bar with a temperature varying between 393K and 443K and for a molar ratio alcohol/O₂ of 21.3 (which corresponds to a 49 NmL/min of O₂ and 5 mL/min of *tert*-amyl alcohol).

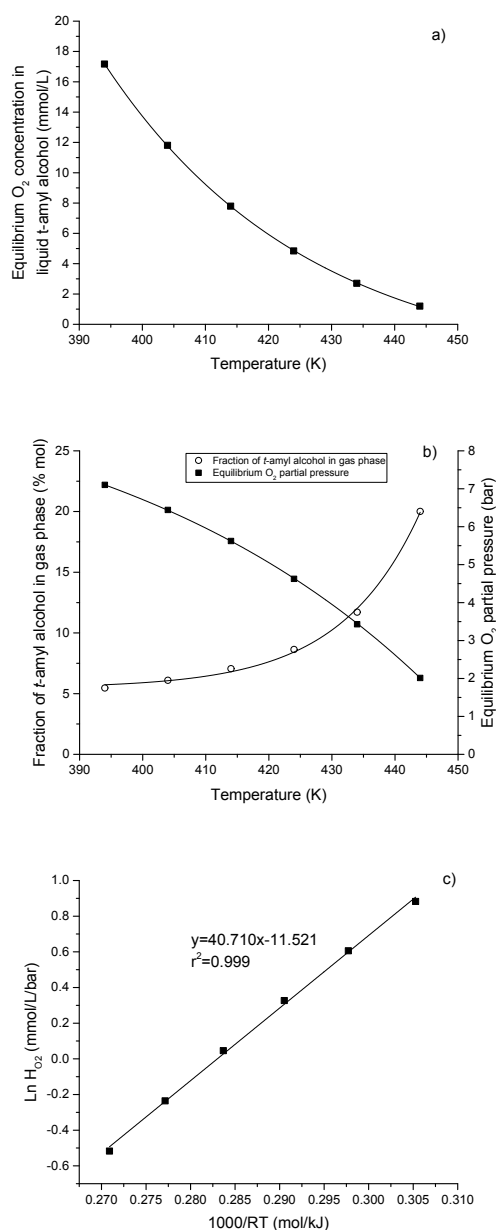


Figure S 2. Typical examples of G-L equilibrium calculations in the binary system O₂ / *tert*-amyl alcohol ($P_{tot} = 9 \text{ bar} - F_{alcohol} / F_{O_2} = 21.28$): (a) Effect of temperature on O₂ solubility; (b) Effect of temperature on O₂ partial pressure and solvent vaporization; (c) corresponding Henry's law.

5. Appreciation of possible mass transfer resistances

The different mass transfer limitations have been evaluated using common chemical engineering approaches regarding the limiting reagent O₂. The physical properties of the gas, liquid and solid phases used in the following calculations are summarized in Table S 1. When necessary (If temperature and/or pressure have an impact), the range of value corresponding to our experimental domain is given.

Table S 1. Considered physical properties of the different phases used in the mass transfer resistance estimations (393K<T<433K and 6bar<P<9bar)

Solid Catalyst/bed			Liquid Phase				Gas phase		
d _p (mm)	e _{cata} (μm)	ε (-)	D _{eff} (10 ⁻¹⁰ m ² /s)	ρ _L (kg/m ³)	μ _L (mPa.s)	σ _L (N/m)	D _{m,L} (10 ⁻⁹ m ² /s)	ρ _G (kg/m ³)	μ _G (10 ⁻⁶ Pa.s)
1.58	100	0.52	2.2 – 2.5	815	0.10 – 0.32	0.021 (at 298K)	1.3 – 1.5	5.3 – 8.8	25.5 – 27.4

a. G-L external mass transfer

G-L mass transfer coefficients, $k_L a_{GL}$, for the different reaction conditions have been evaluated using the correlation established by Zhang et al.⁵ (Eq. 1) for 3-phase milli-packed bed reactors. Depending on the experimental conditions, it varies between 0.5 s⁻¹ and 36 s⁻¹.

$$\frac{k_L a_{GL} d_p^2}{D_{O_2}^L} = 3.41 \times 10^{-5} X_G^{0.08} Re_L^{3.1} We_L^{-1.33} \quad (\text{Eq. 1})$$

Considering the catalyst totally wetted by the liquid phase and the reactor as isothermal, a classical steady state mass balance on O₂ (the limiting reagent) at the different interfaces in a thin layer of the fixed bed (Eq. 2) helps us defining a dimensionless number, " f_{ex}^{GL} " (Eq. 3), analogous the fraction of external mass transfer resistance, " f_{ex} " (Eq. 4), for monofluid/solid cases.

$$k_L a_{GL} (C_{O_2}^* - C_{O_2}^L) = k_S a_{LS} (C_{O_2}^L - C_{O_2, su}^S) = (1 - \varepsilon) \bar{r}_p \quad (\text{Eq. 2})$$

$$f_{ex}^{GL} = \frac{\bar{r}_p (1 - \varepsilon)}{k_L a_{GL} C_{O_2}^*} \quad (\text{Eq. 3})$$

$$f_{ex} = \frac{\bar{r}_p (1 - \varepsilon)}{k_S a_{LS} C_{O_2}^L} = \frac{\bar{r}_p L}{k_S C_{O_2}^L} \quad (\text{Eq. 4})$$

This number compares the apparent rate of reaction on the solid catalyst, $(1 - \varepsilon) \bar{r}_p$, with the highest rate of G-L mass transfer, $k_L a_{GL} C_{O_2}^*$. It has been evaluated at the entrance of the fixed bed where reactant concentrations and where reaction rates are the highest. In all the tested conditions, the f_{ex}^{GL} fractions are always lower than 0.5%, indicating that the G-L mass transfer is efficient and not limiting for this kinetic determination.

b. L-S external mass transfer

Similarly to the G-L interface, the L-S mass transfer coefficients and fractions of L-S external resistances (f_{ex}) have been evaluated for all the reaction conditions at the fixed bed entrance. Here using the correlation of Lakota and Levec⁶ (Eq. 5) developed for multiphase packed beds in low interaction regime under trickling conditions, assuming totally wetted solid catalyst particles again.

$$Sh = \frac{k_s d_p}{D_{m,L}} = 0.487 \frac{1 - \varepsilon}{\varepsilon} \left(Re_L \frac{\varepsilon}{(1 - \varepsilon)(\varepsilon_L - \varepsilon_{Lc})} \right)^{0.495} Sc_L^{0.333} \quad (\text{Eq. 5})$$

The f_{ex} values obtained here are always lower than 0.1%, indicating low and negligible external resistances at the L-S interface.

c. Internal mass transfer

To evaluate the relative impact of internal mass transfer resistance, the classical Weisz criterion³, " ϕ " (Eq. 6), has been used and estimated in all the experiments at the reactor entrance.

$$\phi = \frac{\bar{r}_p L^2}{D_{eff} C_{O_2}^L} \quad (\text{Eq. 6})$$

It is noticeable that the catalyst used in all this study is an egg-shell catalyst with a homogeneously impregnated layer of approximately 300 μm as estimated by optical microscopy (Figure S 2, digital microscope Keyence VHX 6000). Thus, this characteristic length is logically used here.

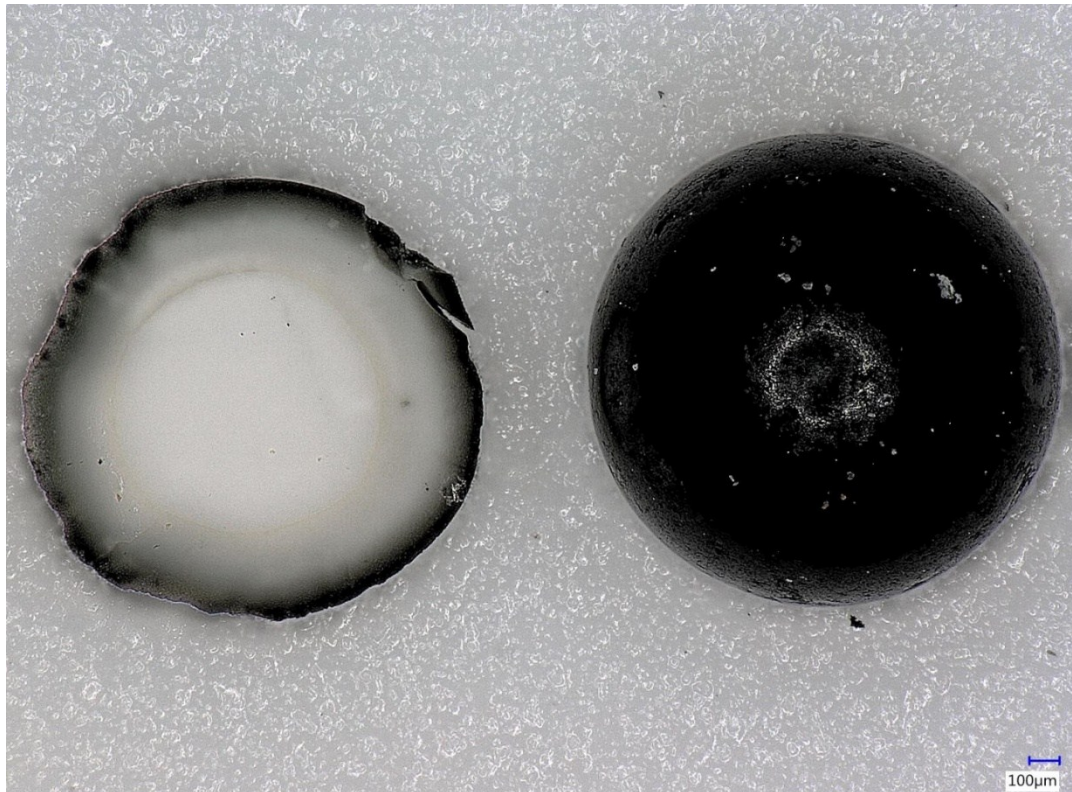


Figure S 3. View of $\text{Ru}^0/\text{Al}_2\text{O}_3$ catalyst particles showing the egg-shell typical structure on a crushed particle (left) and an intact spherical particle (right)

To estimate the effective diffusivity given in Table S 1, classical order of magnitude of liquid diffusivity ($D_{m,L O_2} = 10^{-9} \text{m}^2/\text{s}$ at ambient temperature and pressure), internal porosity ($\beta_p = 50\%$) and tortuosity ($\tau=3$) have been used. Knudsen diffusivity has been neglected (liquid phase wetting the catalyst) and the effect of temperature on $D_{m,L O_2}$ has been taken into account. All the Weisz criterions fall always under a value of 0.06 ($\ll 1$), indicating no appreciable internal mass transfer limitation.

Overall, a work under chemical regime in this reactor has been determined for all the tested conditions, allowing a correct and direct determination of intrinsic kinetic parameters.

6. Determination of adsorption enthalpies through a liquid inverse chromatographic method

The adsorption enthalpies of benzyl alcohol and benzaldehyde (diluted on *tert*-amyl alcohol) on the Ru/Al₂O₃ catalyst were determined using an inverse liquid chromatographic method using pulse injection of each single solute at different temperatures. Precise and constant liquid flowrate of 1.8 mL/min of *tert*-amyl alcohol is applied to the packed catalyst bed with a Shimadzu HPLC pump LC20AD under a pressure of 9 bar and at different temperatures in the range 313-412K. Reproducible pulse injections of a 0.2 mol/L solution of each solute are obtained using a 0.54 mL loop mounted on a switching 6-way valve (Rheodyne 7725i). The resulting transient outlet concentration is recorded on-line at a frequency of 0.5 Hz with a calibrated UV-Vis spectrometer UV5bio from Mettler-Toledo equipped with a quartz cell QS from Hellma Analytics having an internal volume of 80 μL . Mean retention times, t_R are extracted from these measurements through a classical RTD approach with an Excel program. The residence time without adsorption, $t_{R,0}$, has been determined independently with a pulse injection of heptane followed by sampling at the outlet of the reactor each 60s and GC off-line analysis. A value of $t_{R,0}$ of 293s has been determined and is necessary to calculate reduced retention times, t'_R , and the corresponding capacity factors, k' , of the solutes in given conditions according to equations Eq. 7 and Eq. 8 respectively.

$$t'_R = t_R - t_{R,0} \quad (\text{Eq. 7})$$

$$k' = \frac{t'_R}{t_{R,0}} \quad (\text{Eq. 8})$$

Given that that the capacity factor is directly linked to the adsorption equilibrium constant (Eq. 9) and knowing the Van't Hoff thermodynamic relationship (Eq. 10), it is easy to determine the adsorption enthalpy for each solute (Eq. 11):

$$k' = K \frac{V_S}{V_M} \quad (\text{Eq. 9})$$

$$\frac{d(\ln k')}{dT} = \frac{d(\ln K)}{dT} = \frac{\Delta H}{RT^2} \quad (\text{Eq. 10})$$

$$\Delta H = -R \frac{d(\ln k')}{d(1/T)} \quad (\text{Eq. 11})$$

K is defined as the ratio of solute concentrations in the stationary phase and in the mobile phase. V_S and V_M are the volumes of stationary and mobile phases respectively.

The results for both solutes are given in Table S 2 and in Figure S 3.

Table S 2. Experimental enthalpies of adsorption for benzyl alcohol and benzaldehyde on the Ru⁰/Al₂O₃ catalyst of this study.

Species	Benzyl alcohol (A)	Benzaldehyde (B)
Adsorption enthalpies (ΔH_{ads} , kJ/mol)	-22.0	-18.6

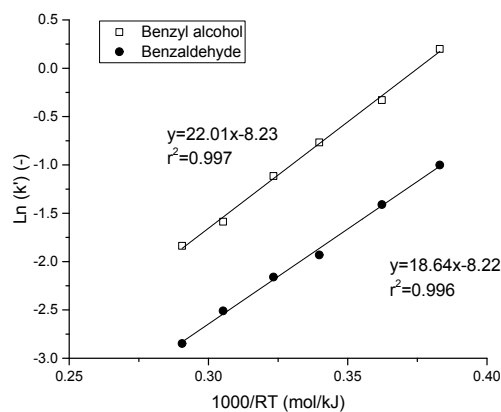


Figure S 4. Graphical determination of adsorption enthalpies of benzyl alcohol and benzaldehyde

7. References

1. M. Selinsek, B. J. Deschner, D. E. Doronkin, T. L. Sheppard, J.-D. Grunwaldt and R. Dittmeyer, *ACS Catal.*, 2018, **8**, 2546-2557.
2. D. W. Flaherty, *ACS Catal.*, 2018, **8**, 1520-1527.
3. N. M. Wilson and D. W. Flaherty, *J. Am. Chem. Soc.*, 2016, **138**, 574-586.
4. Prosim - software and services in process simulation, <http://www.prosim.net/>, (accessed 18-09-2018).
5. J. S. Zhang, A. R. Teixeira and K. F. Jensen, *AIChE J.*, 2018, **64**, 564-570.
6. A. Lakota and J. Levec, *AIChE J.*, 1990, **36**, 1444-1448.